Geol. Mag. **144** (*2*), *2007, pp. 235–246.* © *2007 Cambridge University Press*

doi:10.1017/S0016756806003025 First published online 20 December 2006 *Printed in the United Kingdom*

Precise U–Pb ages of syn-extensional Miocene intrusions in the central Menderes Massif, western Turkey

JOHANNES GLODNY* & RALF HETZEL†

*GeoForschungsZentrum Potsdam, Telegrafenberg C2, 14473 Potsdam, Germany
†Geologisch-Paläontologisches Institut, Universität Münster, Corrensstr. 24, 48149 Münster, Germany

(*Received* 10 February 2006; *accepted* 4 May 2006)

Abstract – Western Turkey is an area which has experienced large-scale extension of continental crust. Here we report precise crystallization ages of two intrusions in the central Menderes Massif, the Turgutlu and Salihli granodiorites, using U–Pb dating. Both intrusions occur in the southern footwall of the seismically active Alaşehir graben and were emplaced syntectonically in an extensional top-to-the-NNE shear zone which was active at retrograde greenschist-facies conditions. The U–Pb ages of 16.1 ± 0.2 Ma (monazite, Turgutlu granodiorite) and 15.0 ± 0.3 Ma (allanite, Salihli granodiorite) document that tectonic exhumation of middle-crustal rocks in the central Menderes Massif was already underway at the Early to Middle Miocene transition. Combined with published geochronological, structural and sedimentological data, the new U–Pb ages point to a continued extension since at least 16 Ma. There is no convincing evidence for a late Miocene/Pliocene phase of tectonic shortening.

Keywords: Turkey, Menderes Massif, extension, granitoids, U–Pb.

1. Introduction

Constraining the age of tectonic events in orogenic belts is notoriously difficult, as accurate isotopic ages for a certain phase of deformation have to be derived from rocks which commonly experienced a complex tectono-metamorphic history. Both the temperature–time path and the deformation history of a rock may be important in resetting an 'isotopic clock' system (e.g. Vance, Müller & Villa, 2003). As ductile deformation of rocks at middle-crustal levels commonly proceeds in the presence of fluids and at temperatures which are in the same range (~ 300–600 °C) as those widely considered as 'closure temperatures' for the K–Ar and Rb–Sr decay systems in micas and amphibole, the interpretation of K–Ar, Ar–Ar and Rb–Sr ages is often problematic. Mandatory for any meaningful age data is complete loss of radiogenic Ar, or complete Sr-isotopic homogenization during deformation. Furthermore, for direct isotopic dating of fault rocks the presence of unaltered (K,Rb)-bearing phases is required, which is not always the case. Even if all preconditions are met, ages for tectonically deformed rocks may, depending on deformation temperatures (Getty & Gromet, 1992), either date the cooling of the rock through a certain temperature interval (in the sense of Dodson, 1973) or may reflect the cessation of ductile deformation (e.g. Beckholmen & Glodny, 2004). Correct interpretation of isotopic age data thus generally requires detailed and laborious microstructural investigations and insights into the spatial distribution of isotopes at the microscale (Reddy & Potts, 1999; Vance, Müller & Villa, 2003).

An alternative to direct isotopic dating of deformation is to date the crystallization of igneous rocks which are syntectonic with respect to a certain phase of deformation (e.g. Pe-Piper, Koukouvelas & Piper, 1998; Ring & Collins, 2005). This is best achieved by U–Pb dating of retentive accessory phases that remain unaffected by the deformation. Here we illustrate this approach by deriving precise U–Pb ages of monazite and allanite, which tightly constrain the age of two granodiorites that intruded an extensional ductile shear zone in the southern footwall of the Alaşehir graben, central Menderes Massif, western Turkey (Fig. 1). The age data shed new light on the continuously disputed timing of extensional deformation in the central Menderes Massif.

2. Geological setting

2.a. Back-arc extension in the Aegean region and related Miocene intrusions

Since the first recognition of extensional shear zones and detachment faults in the back-arc of the Hellenic subduction zone (Lister, Banga & Feenstra, 1984), the tectonic exhumation of metamorphic rocks in the Aegean region has been intensely studied (e.g. Avigad *et al.* 1992; Gautier, Brun & Jolivet, 1993; Bozkurt & Park, 1994; Hetzel *et al.* 1995*a*,*b*; Işik, Seyitoğlu & Çemen, 2003; Ring *et al.* 2003; Kumerics *et al.* 2005). Time constraints for these exhumation processes have been derived from both metamorphic rocks and from abundant Miocene, extension-related

*Author for correspondence: glodnyj@gfz-potsdam.de

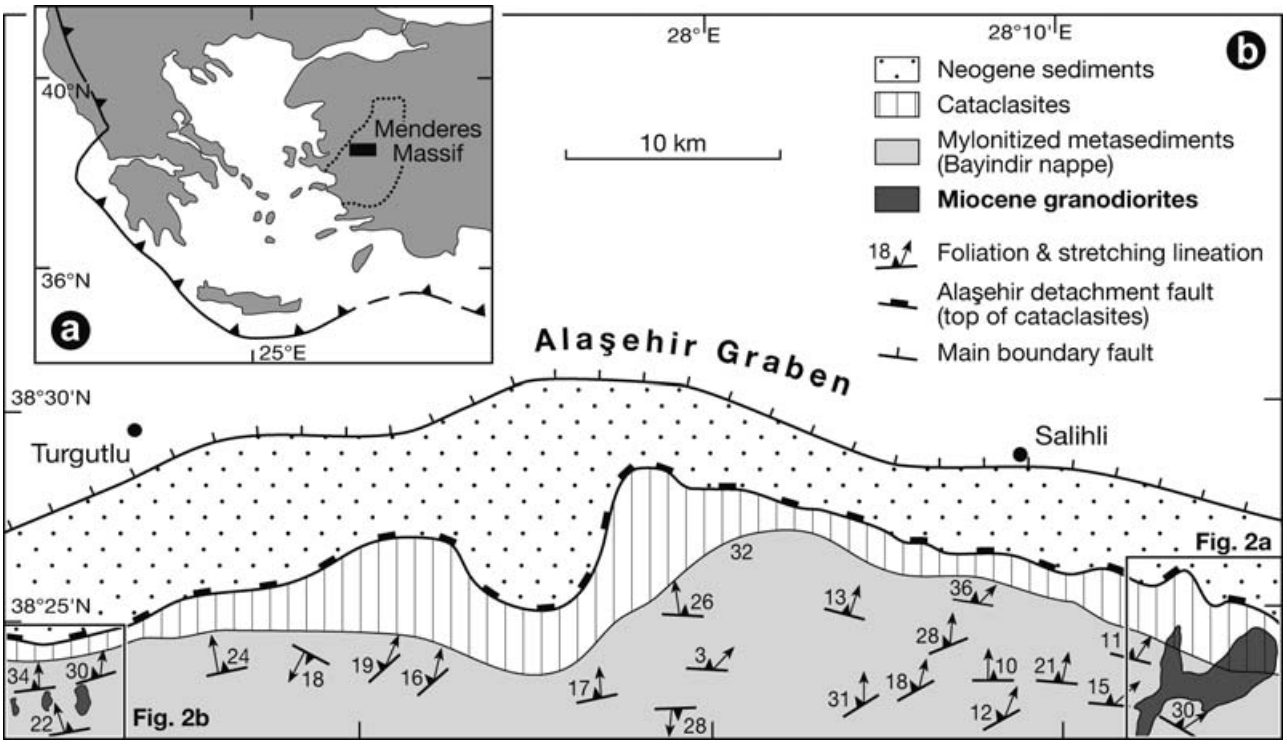

Figure 1. Geological map of the study area, with locations of the Turgutlu and Salihli granodiorites (see Fig. 2a, b). Inset shows the location of the Menderes Massif in the Aegean region.

intrusives. The Miocene intrusions form an arcuate belt in the back-arc of the Hellenic subduction zone (Fig. 1a), stretching from the Greek mainland to the Cycladic archipelago and into western Turkey (e.g. Altherr *et al.* 1982; Yılmaz *et al.* 2001; Altherr & Siebel, 2002). The intrusions are either syntectonic with respect to the extensional deformation, or post-date the ductile fabrics in their country rocks (e.g. Faure, Bonneau & Pons, 1991; Hetzel *et al.* 1995*b*; Pe-Piper, Piper & Matarangas, 2002; Bozkurt, 2004; Işik, Tekeli & Seyitoğlu, 2004; Ring & Collins, 2005; Thomson & Ring, 2006). Most isotopic ages determined for these intrusions are based on the K–Ar and Rb–Sr isotope systems, particularly of mica phases (Altherr *et al.* 1982; Wijbrans & McDougall, 1988; Seyitoğlu, Scott & Rundle, 1992; Hetzel *et al.* 1995*b*; Avigad, Baer & Heimann, 1998; Bröcker & Franz, 1998; Işik, Tekeli & Seyitoğlu, 2004), and in many cases it remains equivocal if the ages date the emplacement of the intrusions, their deformation or their subsequent cooling. U–Pb zircon and/or titanite ages for the intrusions are rare (Henjes-Kunst *et al.* 1988, S. Keay, unpub. Ph.D. thesis, Australian National Univ. Canberra, 1998; Keay, Lister & Buick, 2001; Ring & Collins, 2005). U–Pb zircon dating proved to be difficult due to factors such as the presence of zircon growth zoning or inherited zircon components (e.g. Henjes-Kunst *et al.* 1988). On a regional scale, considering occurrences both in Greece and in western Turkey, available age data for Miocene intrusions cluster roughly between 24 and 10 Ma.

2.b. The Menderes Massif: extension of an Alpine orogen

The Menderes Massif in western Turkey consists of an Alpine nappe pile that was generated during Late Cretaceous/Palaeogene northward subduction of the Neotethys along the Izmir–Ankara suture (Şengör, Satir & Akkök, 1984; Collins & Robertson, 1998; Ring *et al.* 1999; Gessner *et al.* 2001*c*). Parts of the massif have experienced an earlier Pan-African history of metamorphism, magmatism and deformation that is only beginning to be understood (Oberhänsli *et al.* 1997; Loos & Reischmann, 1999; Candan *et al.* 2001; Gessner *et al.* 2001*a*,*c*; Gessner *et al.* 2004). Following Alpine nappe stacking, the whole thrust pile has been extended along a number of extensional shear zones and detachment faults, beginning in late Oligocene to Middle Miocene times (e.g. Bozkurt & Park, 1994; Hetzel *et al.* 1995*a*,*b*; Emre, 1996; Işik & Tekeli, 2001; Gessner *et al.* 2001*b*; Işik, Tekeli & Seyitoğlu, 2004) with the exact timing being a matter of controversy. Apart from tectonic denudation, various sedimentary basins testify that erosion has also played a role in exhuming the metamorphic rocks of the massif (Seyitoğlu, Scott & Rundle, 1992; Seyitoğlu & Scott, 1996; Yılmaz *et al.* 2000; Yılmaz & Gelisli, 2003; Purvis & Robertson, 2004, 2005*a*,*b*; Westaway, 2006). More detailed information on the tectono-metamorphic evolution of the Menderes Massif can be found in a Special Volume of the International Journal of Earth Sciences (Bozkurt & Oberhänsli, 2001), and in Purvis & Robertson (2004 and references therein).

https://doi.org/10.1017/S0016756806003025 Published online by Cambridge University Press

The current extension of the Menderes Massif is concentrated along four E–W-trending graben. The two largest of these graben, the Alaşehir graben (also known as Gediz graben) in the north and the Büyük Menderes graben in the south, are seismically active and separate the central Menderes Massif from a northern and a southern submassif (Şengör, 1987; Cohen *et al.* 1995; Yılmaz *et al.* 2000). A regional reconaissance zircon and apatite fission track study, complemented by a few Ar–Ar ages, revealed that the two outer submassifs of the Menderes Massif had already cooled to below ~ 100 °C by about 20 Ma, whereas the central submassif was still at temperatures above ~ 300 °C (Ring *et al.* 2003). On the basis of these age data and previous structural investigations (Cohen *et al.* 1995; Bozkurt, 2000; Ring *et al.* 2003 and references therein), two periods of extension have been inferred on the scale of the whole massif: the earlier phase led to the exhumation of the two outer submassifs in the late Oligocene/Early Miocene, whereas the central submassif was exhumed later, in Miocene/Pliocene to Recent times (Gessner *et al.* 2001*b*; Ring *et al.* 2003; Bozkurt & Sözbilir, 2004; Seyitoğlu, Işik & Çemen, 2004). The details of the extensional and sedimentary history are far from being resolved, mainly because of the difficulties in establishing an absolute chronology for the continental deposits in the various basins, and the paucity of isotopic age data, which can be tied to the structural evolution of the deformed metamorphic rocks. Considerable debate centres around the exact timing of the extensional episodes, and particularly around a hypothesized intermittent episode of shortening in late Miocene times (e.g. Koçyiğit, Yusufoğlu & Bozkurt, 1999; Yılmaz *et al.* 2000; Seyitoğlu, Çemen & Tekeli, 2000).

In the central Menderes Massif, the metamorphic rocks exposed south of the Alaşehir Graben comprise different metasediments (quartzite, schist, phyllite and marble), which belong to the Bayindir nappe (Ring *et al.* 1999; Gessner *et al.* 2001*a*) (Fig. 1b). The greenschist-facies metasediments have a tectonic foliation parallel to the compositional layering, which dips gently to the north, and a well-developed stretching lineation plunging gently NNE (Hetzel *et al.* 1995*b*; Emre, 1996; Işik, Seyitoğlu & Çemen, 2003; Fig. 1). Abundant kinematic indicators in the mylonites give a consistent top-to-the-NNE shear sense (Hetzel *et al.* 1995*b*; Işik, Seyitoğlu & Çemen, 2003). During decreasing temperatures the mylonites were cataclastically overprinted along a detachment fault (further referred to as Alaşehir detachment, also known as 'Kuzey detachment'), which is associated with a 20 to 50 m thick zone of cataclasite (Fig. 1). At present, the Alaşehir detachment dips ~ 15° N to NE and separates the metamorphic rocks from variably southward-tilted Neogene sediments (Hetzel *et al.* 1995*b*; Purvis & Robertson, 2004).

The crustal-scale ductile shear zone, which records the tectonic denudation of the metamorphic rocks, contains two granodiorite intrusions: the Turgutlu and Salihli granodiorites (Figs 1b, 2). The following arguments, summarized from Hetzel *et al.* (1995*b*), indicate that these granodiorites are syntectonic with respect to the extensional ductile deformation: (1) the mylonitic foliation and stretching lineation have a similar orientation in both the intrusions and their mylonitized host rock (Fig. 2a, b); (2) the mylonitic fabrics in the granodiorites and their country rock formed at similar retrograde greenschist-facies conditions and unequivocally give the same top-to-the-NNE sense of shear; (3) the granodiorite intrusions show no evidence for any deformation earlier than the retrograde greenschist-facies mylonitic foliation, in contrast to the country rocks which experienced an earlier deformation, presumably related to nappe stacking (e.g. Gessner *et al.* 2001*a*); (4) undeformed or little-deformed parts of the Turgutlu granodiorite cross-cut the foliation of the country rock mylonites, indicating that top-to-the-NNE shearing in these parts has only taken place before the intrusion; (5) on the other hand, contact-metamorphic andalusite and muscovite porphyroblasts in other parts of the country rock of the Turgutlu granodiorite are stretched and boudinaged, indicating continued deformation after the intrusion; and (6) some andalusites developed into δ-type clasts again indicating a top-to-the-NNE shear sense.

2.c. Previous geochronological constraints: granodiorites and their host rocks

Ar–Ar dating of two samples from the Turgutlu and Salihli granodiorites (Hetzel *et al.* 1995*b*) has provided the first time constraints on the extensional ductile deformation in the Menderes Massif. Magmatic biotite from the Turgutlu granodiorite has an Ar–Ar plateau age of 13.2 ± 0.2 Ma (1σ), whereas the Salihli granodiorite yielded an Ar–Ar age on biotite of 12.2 ± 0.4 Ma (Hetzel *et al.* 1995*b*). Amphibole from the same sample of the Salihli granodiorite yielded a complex saddle-shaped release spectrum with a minimum step of 17.9 ± 1.0 Ma and a poorly defined ^{40}Ar–^{39}Ar isochron age of 19.5 ± 1.4 Ma (1σ). The biotite ages were originally interpreted to reflect cooling through approximately 300–350 °C, because the samples are essentially undeformed and possess no foliation (Hetzel *et al.* 1995*b*). Further cooling of the Salihli granodiorite is constrained by two zircon and apatite fission track ages of 5.2 ± 0.3 Ma and 1.9 ± 0.4 Ma, respectively (Gessner *et al.* 2001*b*). Another age constraint has been derived from a quartz-rich mylonite with a well-developed mylonitic foliation just below the Alaşehir detachment. Ar–Ar laser-probe experiments on two splits of white mica yielded ages of 6.7 ± 1.1 Ma and 6.6 ± 2.4 Ma

https://doi.org/10.1017/S0016756806003025 Published online by Cambridge University Press

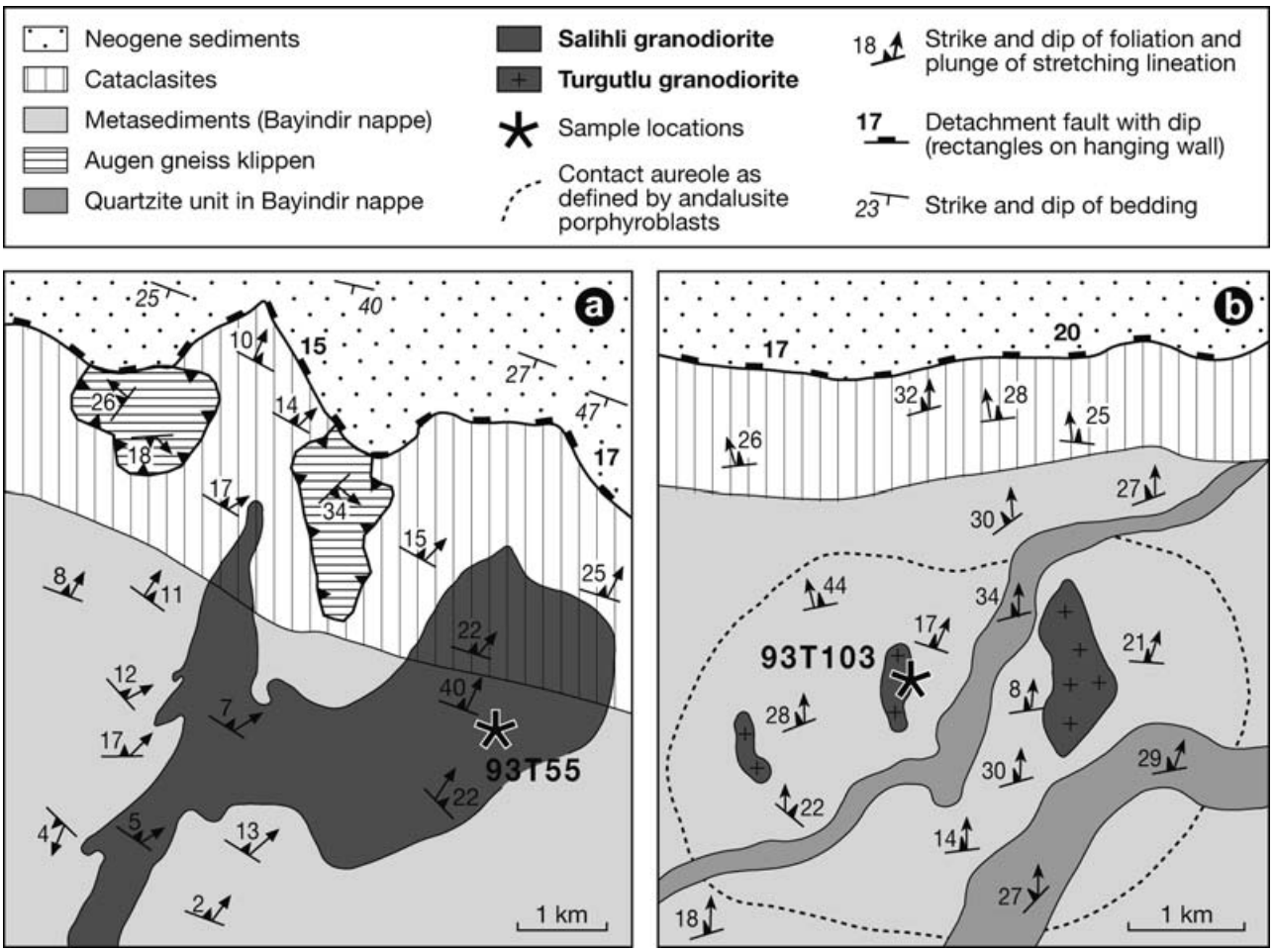

Figure 2. (a) Geological map of the Salihli granodiorite (modified after Hetzel *et al.* 1995*b*). For location, see Figure 1b. (b) Map of the Turgutlu granodiorite (modified after Hetzel *et al.* 1995*b*). For location, see Figure 1b.

(2σ), interpreted as dating deformation and fabric formation at conditions close to the ductile–brittle transition (Lips *et al.* 2001). Matrix monazite grains from metamorphic rocks within the eastern part of the Alaşehir detachment, analysed by ion microprobe, gave ages of 17 ± 5 and 4.5 ± 1.0 Ma, respectively, interpreted to record extension (Catlos & Çemen, 2005).

The above-mentioned 19.5 ± 1.4 Ma amphibole age from the Salihli granodiorite was originally interpreted as the intrusion age of the granodiorite and thus as a minimum age for the onset of extension (Hetzel *et al.* 1995*b*), and has been widely used as an anchor point for regional models on extension, cooling and exhumation (e.g. Seyitoğlu & Scott, 1996; Gessner *et al.* 2001*a*; Lips *et al.* 2001; Purvis & Robertson, 2005*a*,*b*). However, the observed presence of excess Ar within the amphibole has left doubts as to the trustworthiness of the age value (Catlos & Çemen, 2005), and even the interpretation of the age value as dating Miocene granitoid crystallization has been questioned (Westaway, 1996, 2006), which calls for a more reliable determination of the intrusion ages of the two granitoids.

3. Description of the granodiorite samples

Sample 93T55 from the Salihli granodiorite (Fig. 2a) is the same that was analysed by Hetzel *et al.* (1995*b*). The sample is a macroscopically undeformed granitoid, consisting of zoned plagioclase, K-feldspar, quartz, magmatic biotite and amphibole, with traces of apatite, opaques, zircon and allanite. The Turgutlu granodiorite is exposed in three N–S-trending valleys (Fig. 2b). The granodiorite sample 93T103 has been taken from an exposure in the middle valley, where the granodiorite cuts the mylonitic foliation of the country rock schists. The sample exhibits a slight tectonic foliation as well as a weakly developed stretching lineation that has the same N–S direction as the stretching lineation in the country rock, indicating that the intrusion is syntectonic with respect to the ductile deformation of the schists (Hetzel *et al.* 1995*b*). The sample further shows schlieren-like compositional heterogeneities, defined by variable feldspar grain sizes and variable mineral proportions. The assemblage is comprised of quartz, zoned plagioclase, K-feldspar, with traces of apatite, tourmaline, opaques, garnet, rare epidote/allanite and monazite. Both samples

https://doi.org/10.1017/S0016756806003025 Published online by Cambridge University Press

Table 1. Major element data (in wt %) of samples from the Salihli and Turgutlu granodiorites, Menderes Massif

Sample	93T55 Salihli	93T103 Turgutlu
SiO_2	69.82	77.16
TiO_2	0.56	0.14
Al_2O_3	15.36	12.26
Fe_2O_3	3.82	1.11
MnO	0.07	0.01
MgO	1.57	0.01
CaO	4.09	0.91
Na_2O	2.87	3.17
K_2O	3.04	5.01
P_2O_5	0.21	0.07
BaO	0.06	0.02
LOI	1.20	0.73
U (ppm)	2	nd
Th (ppm)	8	nd
Total	102.6	100.6

Analysis of major elements by XRF, of U and Th by ICP-MS. LOI – loss on ignition (1050 °C); nd – not determined.

are high-K, subalkaline granitoids (Table 1). From both intrusions we selected particularly leucocratic, quartz- and K-feldspar-rich variants for isotopic dating, expecting elevated abundances of U, Th and U, Th-bearing trace phases like monazite and allanite. Both samples have been collected structurally well below the zone of hydrothermal alteration and fracturing associated with the Alaşehir detachment. Petrological indications for hydrothermal alteration are virtually absent, implying that all mineral phases of our samples are igneous in origin.

4. Analytical procedures

Mineral concentrates of K-feldspar, monazite (sample 93T103, Turgutlu) and K-feldspar, allanite (sample 93T55, Salihli) were produced, using standard heavy liquid and magnetic separation techniques. Final purification of mineral concentrates was done by hand-picking under a binocular microscope. Turbid grains were excluded from analysis. After washing of the mineral separates in warm, diluted HNO_3 and ultra-clean H_2O, a ^{235}U–^{205}Pb isotopic tracer was added. Minerals were then dissolved in PTFE capsules on a hot plate, using concentrated HF (allanite, feldspar) or HCl (monazite), respectively. Standard HCl, HBr and HNO_3 anion exchange resin techniques were used for chemical separation of U and Pb. U and Pb isotopic analyses were conducted on a Finnigan MAT 262 TIMS instrument at the GeoForschungsZentrum (GFZ) Potsdam. The 2σ reproducibility of the NBS SRM-981 Pb isotopic standard is better than 0.1 % for the $^{206}Pb/^{204}Pb$ and $^{207}Pb/^{204}Pb$ ratios, and corresponding uncertainties in $^{207}Pb/^{206}Pb$ ratios are < 0.06 %. Laboratory procedural blanks are < 25 pg for Pb and < 3 pg for U. Measured isotopic ratios were corrected by 0.11 ± 0.05 % (2σ)/a.m.u. mass fractionation. Data reduction and age calculation were performed using the programs PBDAT (Ludwig, 1993) and Isoplot/Ex (Ludwig, 1999).

5. Results

For sample 93T55 (Salihli granodiorite), the optically homogeneous allanite population was subdivided into different sieve fractions and further differentiated into idiomorphic, fragmented and fractured grains, resulting in five individual fractions of about 15 to 50 grains each. Allanite consistently turned out to contain nearly 1 wt % of Th, associated with U concentrations of only about 200 ppm. The allanite also contains significant amounts of initial common Pb ($\sim$ 20 ppm). Due to this geochemical signature in combination with the young (Miocene) age, the radiogenic departure of allanite Pb from initial Pb isotopic compositions (as given by the feldspar data in Table 2) is small for $^{206}Pb/^{238}U$ ratios, and almost negligible for $^{207}Pb/^{235}U$ ratios (Table 2). U–Pb data for all allanite fractions are identical within limits of error (Fig. 3). The $^{207}Pb^*/^{235}U$ data do not yield precise age information due to their uncertainties (Fig. 3). Geochronological evaluation of the $^{206}Pb^*/^{238}U$ data involves correction of the possible presence of excess ^{206}Pb. As pointed

Table 2. U–Pb analytical results, Salihli granodiorite (Sample 93T55)

Analysis	Fractions[a]	Weight (mg)	U (ppm)	Pb_{total}[b] (ppm)	$^{206}Pb/^{204}Pb$[c]	$^{207}Pb/^{204}Pb$[c]	$^{208}Pb/^{204}Pb$[c]	$^{206}Pb/^{238}U$[d]	$\pm 2\sigma$ (%)	$^{207}Pb/^{235}U$[d]	$\pm 2\sigma$ (%)	^{206}Pb–^{238}U age (Ma)	^{206}Pb–^{238}U age (Ma) corr.[e]	^{207}Pb–^{235}U age (Ma)
PS942	feldspar	2.442	1.11	34.9	18.87	15.72	39.16	–	–	–	–	–	–	–
PS938	all 125–250	1.040	203	19.4	21.87	15.83	91.84	0.00254	3.41	0.01271	93.1	16.35	14.96	12.83
PS939	all 125–250 fr	0.834	178	17.2	21.95	15.84	95.94	0.00256	3.34	0.01351	86.2	16.45	14.97	13.62
PS940	all 125–250 idi	0.810	204	19.7	21.90	15.86	92.12	0.00259	3.39	0.01619	73.8	16.65	15.22	16.31
PS941	all impure	2.412	188	19.8	21.46	15.80	86.72	0.00254	3.95	0.01108	123	16.33	14.88	11.20
PS943	all > 200 idi	1.366	197	21.42	21.37	15.82	84.51	0.00256	4.10	0.01426	101	16.50	15.03	14.38

[a] Codes in the fraction numbers are: all – allanite. Abbreviations are: 30–100 = size fractions (μm); idi – idiomorphic; fr – fragments.
[b] Total common Pb in sample (initial Pb + blank).
[c] Raw data, corrected for fractionation, and common lead in spike.
[d] Corrected for fractionation, procedural laboratory blanks (< 25 pg Pb, 3 pg U), and initial common Pb (as calculated from PS942 feldspar data). Pb fractionation correction is 0.11%/amu ($\pm$ 0.05% 2σ). 2σ uncertainties on the isotopic ratios are calculated with the error propagation procedure of Ludwig (1980).
[e] Ages corrected for excess ^{206}Pb due to initial ^{230}Th disequilibria, using algorithm of Schärer (1984).

https://doi.org/10.1017/S0016756806003025 Published online by Cambridge University Press

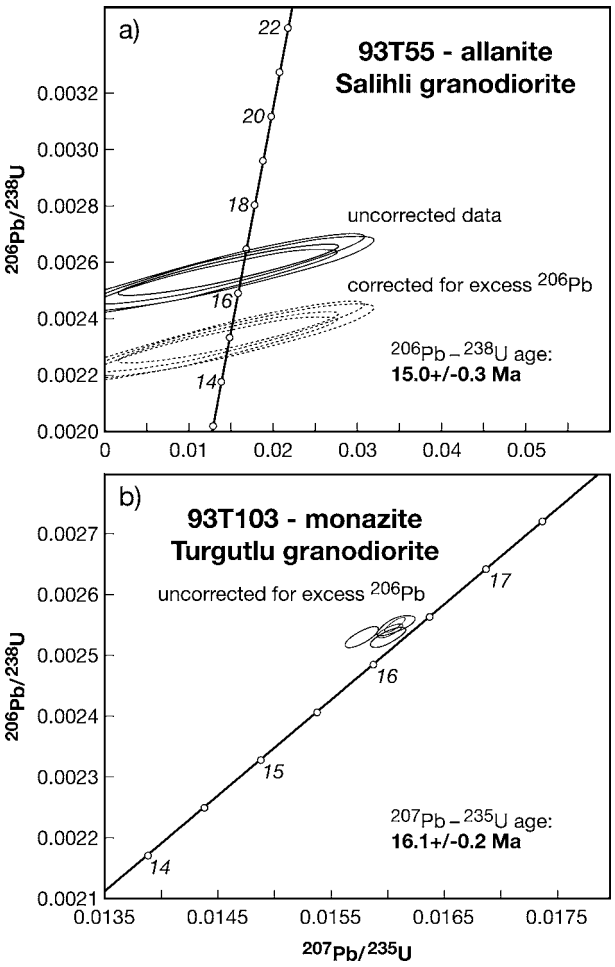

Figure 3. Concordia diagrams for (a) allanite from the Salihli granodiorite, and (b) for monazite from the Turgutlu granodiorite. See Tables 2 and 3 for the analytical data; see text for details on excess ^{206}Pb correction. Allanite ages in (a) have been calculated from excess-^{206}Pb-corrected ^{206*}Pb/^{238}U data, and monazite ages in (b) from ^{207}Pb*/^{235}U data.

out by Schärer (1984), U and Th fractionation between a crystallizing Th-rich mineral and its parent magma may result in U decay series disequilibrium and in initial excess ^{230}Th, leading to excess ^{206}Pb in that mineral. This excess ^{206}Pb can be quantified and corrected for if the Th/U ratios of both the mineral and the parent magma are known (Schärer, 1984). After calculating the Th concentrations of the allanite fractions from their thorogenic ^{208}Pb (Table 2) and using the whole rock Th and U concentrations (Table 1), we obtained excess-^{206}Pb-corrected ^{206}Pb*–^{238}U ages of around 15 Ma for all allanite fractions (Table 2, Fig. 3). Considering potential uncertainties from the correction of excess ^{206}Pb as well as the analytical uncertainties on ^{206}Pb/^{238}U ratios, we arrive at a weighted average ^{206}Pb–^{238}U allanite age of 15.0 ± 0.3 Ma.

From sample 93T103 (Turgutlu granodiorite), monazite was separated into five different fractions, after grain size criteria and according to presence or absence of inclusions. The obtained ^{206}Pb*–^{238}U ages are systematically higher than corresponding ^{207}Pb*–^{235}U ages (Table 3), resulting in reverse discordance in a ^{206}Pb*/^{238}U–^{207}Pb*/^{235}U diagram (Fig. 3). This effect can again be explained by the presence of excess ^{206}Pb (Schärer, 1984), as typical for geologically 'young' monazite and allanite. In the case of the monazite of this sample, we did not correct ^{206}Pb*–^{238}U ages for excess ^{206}Pb, since no truly representative whole rock sample was available because of the lithological heterogeneity of the sample. Instead, the initial U/Pb ratios of monazite were sufficiently high to allow for derivation of precise ^{207}Pb*–^{235}U ages even for these young monazites. Four out of our five analyses are identical within 2σ-limits of error, while one appears to be slightly younger (Fig. 3). Calculation of Tukey's biweight mean, incorporating all monazite analyses, leads to an ^{207}Pb*–^{235}U age of 16.1 ± 0.2 Ma (2σ) for the monazite population.

6. Discussion

6.a. Interpretation of U–Pb geochronological data

The U–Pb system of monazite is generally considered as a fairly robust geochronometer, suitable for dating granitoid crystallization (e.g. Copeland, Parrish & Harrison, 1988). In fact, the U and Pb volume diffusion characteristics of monazite almost inhibit any diffusional resetting of the U–Pb system of monazite even at temperatures of granite crystallization (Cherniak *et al.* 2004). The post-crystallizational metamorphic history recorded in our nearly undeformed sample of the Turgutlu granodiorite gives no indications for either metamorphic or hydrothermal monazite growth, or for non-diffusional age reset mechanisms like dissolution–reprecipitation or recrystallization. Any significant reset of monazite ages after monazite crystallization would probably also manifest in a major spread of data for different grain size fractions in a ^{206}Pb*/^{238}U–^{207}Pb*/^{235}U diagram, which is not observed (Fig. 3). The ^{207}Pb/^{235}U system in monazite is, unlike the ^{206}Pb/^{238}U system, not subject to major systematic effects from possible initial U decay series disequilibria (cf. Schärer, 1984). We therefore interpret the monazite ^{207}Pb–^{235}U ages as dating crystallization of the Turgutlu granodiorite at 16.1 ± 0.2 Ma.

As to the interpretation of the Salihli-intrusion allanite data, Romer & Siegesmund (2003) have shown that this mineral may, even in magmatic rocks, inherit radiogenic Pb from its precursor phases. Such inheritance would result in discordant data in a ^{206}Pb*/^{238}U–^{207}Pb*/^{235}U diagram. However, our dataset does not show any evidence for isotopic inheritance as all allanite data are identical and concordant within limits of error. Pb and U volume diffusion in allanite does not occur to any significant extent at temperatures comparable to temperatures of granitoid crystallization (~ 700 °C; cf. Oberli *et al.* 2004). We therefore interpret

https://doi.org/10.1017/S0016756806003025 Published online by Cambridge University Press

Table 3. U–Pb analytical results, Turgutlu granodiorite (Sample 93T103)

Analysis	Fraction	Weight (mg)	U (ppm)	Pb_{total} (ppm)	Pb_{com} [b] (ppm)	$^{206}Pb/^{204}Pb$ [c]	$^{208}Pb/^{206}Pb$ [d]	$^{206}Pb/^{238}U$ [d]	$\pm 2\sigma$ (%)	$^{207}Pb/^{235}U$ [d]	$\pm 2\sigma$ (%)	$^{207}Pb/^{206}Pb$ [d]	$\pm 2\sigma$ (%)	$^{206}Pb–^{238}U$ age (Ma)	$^{207}Pb–^{235}U$ age (Ma)	$^{207}Pb–^{206}Pb$ age (Ma)	$\pm 2\sigma$ [e]	Correl. coeff. [f]
PS935	feldspar	1.54	1.87	64.5	–	18.87	2.072 [c]	–	–	–	–	0.83285 [c]	0.05	–	–	–	–	
PS932	mo 40–63 incl	0.172	6489	43.8	1.73	636.8	1.896	0.00255	0.46	0.01604	0.60	0.04563	0.38	16.41	16.15	−22.1	9.1	0.782
PS933	mo 40–63 incl	0.196	5326	37.4	1.22	737.3	2.048	0.00254	0.38	0.01604	0.51	0.04577	0.33	16.36	16.15	−14.7	7.9	0.769
PS934	mo >100 cl incl	0.119	6319	53.1	1.47	725.7	2.661	0.00255	0.44	0.01612	0.67	0.04585	0.48	16.42	16.24	−10.3	12	0.695
PS936	mo 63–100 cl	0.053	6110	41.0	1.32	773.4	1.919	0.00253	0.55	0.01601	0.79	0.04583	0.54	16.31	16.13	−11.1	13	0.739
PS937	mo 63–100 cl	0.124	8394	66.8	2.01	702.0	2.481	0.00253	0.56	0.01578	0.74	0.04520	0.46	16.30	15.90	−44.8	11	0.778

[a] Codes in the fraction numbers are: mo – monazite. Abbreviations are: 30–100 = size fractions (μm); incl – with inclusions; cl – clear.
[b] Total common Pb in sample (initial Pb + blank).
[c] Raw data, corrected for fractionation, and common lead in spike.
[d] Corrected for fractionation, procedural laboratory blanks (< 25 pg Pb, 3 pg U), and initial common Pb (as calculated from PS935 feldspar data). Pb fractionation correction is 0.11%/amu (± 0.05% 2σ). 2σ uncertainties on the isotopic ratios are calculated with the error propagation procedure of Ludwig (1980).
[e] Absolute error, in Ma.
[f] $^{207}Pb/^{235}U$ / $^{206}Pb/^{238}U$ error correlation coefficient.

the allanite U–Pb isotopic data as dating allanite crystallization, contemporaneous with crystallization of the Salihli granodiorite, at 15.0 ± 0.3 Ma.

6.b. Re-evaluation of previous Ar–Ar data

The new allanite U–Pb data from the Salihli granodiorite provide a reliable crystallization age of 15.0 ± 0.3 Ma. This age is significantly younger than the previously determined Ar–Ar amphibole isochron age of 19.5 ± 1.4 Ma (1σ; Hetzel *et al.* 1995*b*). We attribute this age difference to an incomplete correction for excess Ar in the amphibole, which renders the Ar–Ar age geologically meaningless.

In contrast, Ar release spectra for biotite from both the Turgutlu and Salihli granodiorites did not show any indications for excess Ar, and we regard the Ar–Ar plateau ages obtained by Hetzel *et al.* (1995*b*) of 13.1 ± 0.2 Ma for Turgutlu biotite and of 12.2 ± 0.4 Ma for Salihli biotite as dating Ar-isotopic closure of the biotite. Both biotite samples did not experience any post-crystallizational deformation (we note that the biotite sample from the Turgutlu granodiorite analysed by Hetzel *et al.* (1995*b*) was not the slightly deformed sample 93T103 but a completely undeformed one). Synkinematic recrystallization can thus be ruled out as an age-resetting mechanism. Therefore, Ar isotopic closure is possibly related to cooling to temperatures below ∼450 °C (cf. Villa, 1998; Villa & Puxeddu, 1994). However, as we have no information on presence, properties, or absence of intergranular aqueous fluids at the time of biotite isotopic closure, we cannot rule out that in fact a kind of fluid-aided resetting is dated. Hydrothermal Ar bulk loss experiments on biotite point to isotopic closure at temperatures of ∼350–300 °C (e.g. Grove & Harrison, 1996). In consequence, we can only state that the biotite Ar–Ar 'clock' was set at temperature conditions between ∼450 and ∼300 °C. Interestingly, there is a systematic difference in age between our new U–Pb crystallization ages and the Ar–Ar biotite ages for the two intrusions. Both biotite Ar–Ar ages are ∼3 Myr 'younger' than the corresponding U–Pb crystallization ages (13.1 ± 0.2 Ma v. 16.1 ± 0.2 Ma for the Turgutlu body, and 12.2 ± 0.4 Ma v. 15.0. ± 0.3 Ma for the Salihli granitoid, respectively). Therefore, although the Ar–Ar biotite ages cannot be tied to a precise temperature, they indicate that the roof zone of the two granitoids was at temperatures high enough (> 300 °C) to facilitate ductile deformation for at least 3 Myr following the intrusion of the granodiorites. According to thermal models for comparable granitic bodies (e.g. Coulson *et al. 20*02), thermal relaxation of fairly small granitoid bodies is expected to be nearly complete after 3 Myr (the time span between granite crystallization and the corresponding Ar–Ar biotite ages). Therefore, it is likely that temperatures of > 300 °C prevailed for at least 3 Myr after granitoid intrusion (until 13/12 Ma),

https://doi.org/10.1017/S0016756806003025 Published online by Cambridge University Press

not only in the granitoids but also in the country rocks in the present-day level of exposure.

Estimating the present-day geothermal gradient in the upper crust from the average present-day heat flow in western Anatolia (Ilkişik, 1995) and standard heat flow models for continental crust (Chapman & Furlong, 1992) suggests a regional geothermal gradient of $\sim 40\,^{\circ}$C/km. Using the temperature value of 300 °C for Ar-isotopic closure of the biotites, this gradient leads to a minimum amount of exhumation of 7.5 km since *c.* 13–12 Ma. We note that the geothermal gradient has likely increased with time, owing to the advective heat transport during crustal extension, which again suggests that the exhumation estimate is a minimum. The growth of andalusite porphyroblasts in the contact aureole of the Turgutlu granodiorite may be used to place an upper limit on the intrusion depth and thus the total amount of exhumation of the Turgutlu granodiorite. The Al_2SiO_5 triple point is located at pressures of 3.5 to 4.5 kbar in *PT*-space (e.g. Larson & Sharp, 2003 and references therein), which corresponds to crustal depths of 13 to 17 km, respectively. In conclusion, we estimate that 10–15 km of overburden has been removed in the last 15–16 Myr by a combination of tectonic extension and erosion at the surface.

6.c. Implications for the timing of extension in the central Menderes Massif

Contact relationships and deformation patterns of the Turgutlu and Salihli granodiorites and their host rocks suggest that the granitoids intruded into already mylonitized country rocks and experienced shearing at retrograde greenschist-facies conditions. In other words, the granodiorites are syntectonic with respect to the top-to-the-NNE extensional shear zone exposed in the southern footwall of the Alaşehir graben. Our new crystallization ages for the two intrusions therefore imply that extension in this part of the central Menderes Massif was already underway at 16.1 ± 0.2 Ma. It is an open question whether regional magmatism was temporally nearly coincident with the formation of extension-related ductile shear zones, or whether there has been a significant time gap between early extensional deformation and incipient regional magmatism. The Neogene sediments along the southern and northern margin of the Alaşehir graben may be used to shed some light on this question. The variably southward-tilted sediments along the southern margin of the graben rest upon the Alaşehir detachment fault. For the lower portion of the sedimentary succession a sporomorph assemblage suggests an Early to Middle Miocene age (*c.* 20–14 Ma, Burdigalian to middle–Serravallian: Seyitoğlu & Scott, 1996; Seyitoğlu *et al.* 2002), although some workers argue for a Late Miocene age (e.g. Yılmaz *et al.* 2000 and references therein). At the northern margin of the eastern Alaşehir graben near Toygarli (~ 20 km E of Salihli), clastic sediments post-date andesitic lavas with ages between 14.0 ± 0.4, 14.65 ± 0.06, and 16.1 ± 0.9 Ma, obtained by K–Ar and Ar–Ar methods using biotite and amphibole (Ercan *et al.* 1997; Purvis & Robertson, 2004, 2005*a*,*b*). According to Cohen *et al.* (1995), the volcanic rocks near Toygarli coincide temporally with the earliest sediments of the Alaşehir graben. If the oldest sediments along the Alaşehir graben date the initiation of normal faulting, they suggest an age of *c.* 20–15 Ma for the beginning of extensional deformation in the central Menderes Massif.

Several studies in an analogous extension-dominated setting, the Basin and Range province of North America, suggest a strong correlation between the onset of magmatism and the onset of regional extension. In the Basin and Range, volcanism was found to initiate synchronously with the initiation of surface-breaking normal faults (e.g. Armstrong & Ward, 1991; Rahl, McGrew & Foland, 2002). A close correlation between initiation of magmatism and extensional deformation has also emerged for the northernmost part of the Menderes Massif. Here, the large-scale extensional Simav detachment fault operated between *c.* 25 and *c.* 19 Ma, as deduced from zircon fission track data (Thomson & Ring, 2006), U–Pb zircon data for the synkinematic Eğrigöz and Koyunoba granites (21.3–20.1 Ma: Ring & Collins, 2005), and an Ar–Ar mylonitization age of 22.86 ± 0.47 Ma obtained from muscovite (Işik, Tekeli & Seyitoğlu, 2004). The onset of faulting appears to be synchronous with the onset of magmatism, as evident from an U–Pb zircon SIMS age of 24.4 ± 0.3 Ma for a local leucogranitic dyke (Ring & Collins, 2005). By analogy, we hypothesize that extensional deformation in the footwall of the Alaşehir detachment did not substantially pre-date the intrusion of the dated granitoids, that is, extension in the central Menderes Massif may have started *c.* 18–16 Ma ago, in late Burdigalian times.

6.d. Continuous extension since *c.* 16 Ma?

Based on the microtextural evidence from the greenschist-facies shear zone and the gradual transition from the mylonites into the overlying cataclasites of the Alaşehir detachment, Hetzel *et al.* (1995*b*) and Emre (1996) have inferred a more or less continuous N–S- to NNE–SSW-directed extension since the intrusion of the Turgutlu and Salihli granodiorites. In conflict with this interpretation, a short-lived contractional event with N–S-directed shortening in the Pliocene has been inferred by Koçyiğit, Yusufoğlu & Bozkurt (1999), on the basis of folds present in the Neogene sediments along the Alaşehir graben. The evidence presented remains equivocal, however, as Seyitoğlu, Çemen & Tekeli (2000) have demonstrated that the folds in question are likely extensional in origin and do

https://doi.org/10.1017/S0016756806003025 Published online by Cambridge University Press

not indicate crustal shortening. Likewise, N–S-trending fold axes in Miocene sediments south of the Alaşehir graben, which have been interpreted to indicate a Late Miocene compressional phase (Gokten, Havazoğlu & Şan, 2001; Bozkurt, 2003), do not necessarily indicate crustal shortening. We add that Paton (1992), studying normal faulting and sedimentation near Alaşehir, has not reported any evidence for a short-lived contractional event and that Purvis & Robertson (2004) suspect that local tilting and folding in the Usak-Güre basin northeast of the Alaşehir graben are extension-related.

A prolonged phase of N–S- to NNE–SSW-directed extension since at least 16 Ma is also indicated by geochronological data on the post-Serravallian deformation, cooling and exhumation history of the metamorphic rocks south of the Alaşehir graben. First, the results of Ar–Ar laser-probe experiments on white mica from shear zones of the southern Alaşehir graben flank (Alaşehir detachment; 6.7 ± 1.1 Ma and 6.6 ± 2.4 Ma: Lips *et al.* 2001) were interpreted as dating deformation and fabric formation at conditions close to the ductile–brittle transition. A 4.5 ± 1.0 Ma U–Pb monazite age from the Alaşehir detachment (Catlos & Çemen, 2005) was likewise interpreted to record extension, probably by way of synkinematic monazite-forming retrograde reactions. The final cooling of the metamorphic rocks and the granodiorite intrusions is recorded by two fission track ages on zircon (5.2 ± 0.3 Ma) and apatite (1.9 ± 0.4 Ma) (Gessner *et al.* 2001*b*).

Whether the extensional deformation occured in a continuous fashion or in distinct pulses separated by periods of tectonic quiescence cannot be decided with the available geochronological data. On the basis of sedimentological data from the Alaşehir graben, Purvis & Robertson (2004) have argued for two extension pulses with a phase of tectonic quiesence in the Late Miocene. The main evidence for these two extensional phases is a regional unconformity in the sediments along the southern margin of the Alaşehir Graben, separating a Middle Miocene succession deposited by axial fluvial transport from Pliocene alluvial fan deposits recording a transverse transport direction (Purvis & Robertson, 2004). However, such an unconformity may also be related to a change in base level (indeed, a regional surface uplift of about 250 m in the Pliocene has been inferred by Westaway *et al.* (2004)) or to the initiation of a second set of normal faults along the southern margin of the Alaşehir graben (Seyitoğlu *et al.* 2002).

In any case, the Quaternary sediments in the present-day Alaşehir graben, a pronounced seismic activity (e.g. Eyidoğan, 1988), earthquake focal mechanisms (for instance, those reported for the 1969 Alasehir earthquake: Eyidoğan & Jackson, 1985) and GPS data (McClusky *et al.* 2000) demonstrate an ongoing N–S extension in both the Menderes Massif and western Turkey as a whole.

Westaway (2006) has tried to explain the Oligocene/Miocene cooling histories in the Menderes Massif by erosion and flat-slab subduction and states that extension began only *c.* 11 Ma ago, with most of the extension being younger than *c.* 7 Ma. We argue that abundant mylonites and syntectonic intrusions present in different parts of the Menderes Massif and their progressive deformational overprint at decreasing temperatures, in combination with geochronological data derived from these rocks, indicate that continental extension started much earlier (Hetzel *et al.* 1995*b*; Işik & Tekeli, 2001; Işik, Seyitoğlu & Çemen, 2003; Ring *et al.* 2003; Işik, Tekeli & Seyitoğlu, 2004; Ring & Collins, 2005; Thomson & Ring, 2006; this study).

7. Conclusions

Our new U–Pb ages of 16.1 ± 0.2 Ma (monazite, Turgutlu granodiorite) and 15.0 ± 0.3 Ma (allanite, Salihli granodiorite) are high-precision age determinations for crystallization of these intrusive bodies in the central Menderes Massif. The data represent an anchor point for constraining the magmatic and deformation history of the Menderes Massif, and supersede previous widely used but inaccurate amphibole Ar–Ar age data for these granitoids.

Existing biotite Ar–Ar ages date Ar-isotopic closure of biotite at 450–300 °C at about 3 Myr after crystallization of the respective granitoids. This indicates that temperatures were high enough to facilitate ductile extensional deformation of the granitoids and their country rocks until *c.* 13–12 Ma. Petrological considerations lead us to estimate a total exhumation of 10–15 km since granitoid crystallization at 16.1 and 15.0 Ma, respectively. Using 300 °C as the temperature of biotite isotopic closure and an estimated geothermal gradient of ~ 40 °C/km, we arrive at a *minimum* amount of exhumation of 7.5 km since *c.* 13–12 Ma, which must have been accomplished by a combination of tectonic extension and erosion.

The new U–Pb ages, combined with published sedimentological data for the Alaşehir graben deposits and age data for other regional magmatic rocks, indicate that incipient extensional faulting in the central Menderes Massif may be temporally close to granitoid intrusion, that is, late Burdigalian (*c.* 18–16 Ma) in age.

Acknowledgements. Early parts of this work were funded by the Deutsche Forschungsgemeinschaft (DFG). We thank the GFZ Potsdam for continuous support, S. Sindern (RWTH Aachen) for providing geochemical data and V. Kuntz, J. Herwig and M. Dziggel for help with figure drawing and mineral separation. Detailed and constructive reviews by K. Gessner and G. Seyitoğlu, as well as editorial comments by D. Pyle, are gratefully acknowledged.

References

ALTHERR, R., KREUZER, H., WENDT, I., LENZ, H., WAGNER, G. H., KELLER, J., HARRE, W. & HÖHNDORF, A. 1982. A

late Oligocene/early Miocene high temperature belt in the Attic-Cycladic crystalline complex (SE Pelagonian, Greece). *Geologisches Jahrbuch* **E23**, 97–164.

ALTHERR, R. & SIEBEL, W. 2002. I-type plutonism in a continental back-arc setting: Miocene granitoids and monzonites from the central Aegean Sea, Greece. *Contributions to Mineralogy and Petrology* **143**, 397–415.

ARMSTRONG, R. L. & WARD, P. 1991. Evolving geographic patterns of Cenozoic magmatism in the North-American Cordillera: the temporal and spatial association of magmatism and metamorphic core complexes. *Journal of Geophysical Research* **96**, 13201–24.

AVIGAD, D., BAER, G. & HEIMANN, A. 1998. Block rotation and continental extension in the central Aegean Sea: Palaeomagnetic and structural evidence from Tinos and Mykonos (Cyclades, Greece). *Earth and Planetary Science Letters* **157**, 23–40.

AVIGAD, D., MATTHEWS, A., EVANS, B. W. & GARFUNKEL, Z. 1992. Cooling during the exhumation of a blueschist terrane: Sifnos (Cyclades), Greece. *European Journal of Mineralogy* **4**, 619–34.

BECKHOLMEN, M. & GLODNY, J. 2004. Early Cambrian blueschist facies metamorphism in the Kvarkush metamorphic basement, northern Urals, Russia. In *The Neoproterozoic Timanide Orogen of Eastern Baltica* (eds D. G. Gee, V. L. Pease), pp. 125–34. Geological Society of London, Memoir no. 30.

BOZKURT, E. 2000. Timing of extension on the Büyük Menderes Graben, western Turkey, and its tectonic implications. In *Tectonics and magmatism in Turkey and surrounding regions* (eds E. Bozkurt, J. A. Winchester and J. D. A. Piper), pp. 385–403. Geological Society of London, Special Publication no. 173.

BOZKURT, E. 2003. Origin of NE-trending basins in western Turkey. *Geodinamica Acta* **16**, 61–81.

BOZKURT, E. 2004. Granitoid rocks of the southern Menderes Massif (southwestern Turkey): field evidence for Tertiary magmatism in an extensional shear zone. *International Journal of Earth Sciences (Geologische Rundschau)* **93**, 52–71.

BOZKURT, E. & OBERHÄNSLI, R. 2001. Menderes Massif (Western Turkey): structural, metamorphic and magmatic evolution – a synthesis. *International Journal of Earth Sciences* **89**, 679–708.

BOZKURT, E. & PARK, R. G. 1994. Southern Menderes Massif: an incipient metamorphic core complex in western Anatolia, Turkey. *Journal of the Geological Society, London* **151**, 213–16.

BOZKURT, E. & SÖZBILIR, H. 2004. Tectonic evolution of the Gediz graben: field evidence for an episodic, two-stage extension in western Turkey. G*eological Magazine* **141**, 63–79.

BRÖCKER, M. & FRANZ, L. 1998. Rb–Sr isotope studies on Tinos Island (Cyclades, Greece): additional time constraints for metamorphism, extent of infiltration-controlled overprinting and deformational activity. *Geological Magazine* **135**, 369–82.

CANDAN, O., DORA, O. O., OBERHÄNSLI, R., ÇETINKAPLAN, M., PARTZSCH, J. H., WARKUS, F. C. & DÜRR, S. 2001. Pan-African high-pressure metamorphism in the Precambrian basement of the Menderes Massif, western Anatolia, Turkey. *International Journal of Earth Sciences* **89**, 793–811.

CATLOS, E. J. & ÇEMEN, I. 2005. Monazite ages and the evolution of the Menderes Massif, western Turkey. *International Journal of Earth Sciences* **94**, 204–217.

CHAPMAN, D. S. & FURLONG, K. P. 1992. Thermal state of the continental lower crust. In *Continental lower crust* (eds D. M. Fountain, R. Arculus and R. W. Kay), pp. 179–99. Elsevier: Amsterdam.

CHERNIAK, D. J., WATSON, E. B., GROVE, M. & HARRISON, T. M. 2004. Pb diffusion in monazite: a combined RBS/SIMS study. *Geochimica et Cosmochimica Acta* **68**, 829–40.

COHEN, H. A., DART, C. J., AKYÜZ, H. S. & BARKA, A. 1995. Syn-rift sedimentation and structural development of Gediz and Büyük Menderes Grabens, western Turkey. *Journal of the Geological Society, London* **152**, 629–38.

COLLINS, A. S. & ROBERTSON, A. H. F. 1998. Processes of Late Cretaceous to Late Miocene episodic thrust sheet translation in the Lycian Taurides, SW Turkey. *Journal of the Geological Society, London* **155**, 759–72.

COPELAND, P., PARRISH, R. R. & HARRISON, T. M. 1988. Identification of inherited radiogenic Pb in monazite and its implications for U–Pb systematics. *Nature* **333**, 760–3.

COULSON, I. M., VILLENEUVE, M. E., DIPPLE, G. M., DUNCAN, R. A., RUSSELL, J. K. & MORTENSEN, J. K. 2002. Time-scales of assembly and thermal history of a composite felsic pluton: constraints from the Emerald Lake area, northern Canadian Cordillera, Yukon. *Journal of Volcanology and Geothermal Research* **114**, 331–56.

DODSON, M. H. 1973. Closure temperature in cooling geochronological and Petrological Systems. *Contributions to Mineralogy and Petrology* **40**, 259–74.

EMRE, T. 1996. The tectonic evolution of the Gediz graben. *Geological Bulletin of Turkey* **39**, 1–18.

ERCAN, T., SATIR, M., SEVIN, D. & TÜRKECAN, A. 1997. Bati Anadolu'daki Tersiyer ve Kuvarterner yağlikayaçlarda yeni yapilan radyometrik yaş ölçümlerinin yorumu. *MTA Bulletin* **119**, 103–12.

EYIDOĞAN, H. 1988. Rates of crustal deformation in western Turkey as deduced from major earthquakes. *Tectonophysics* **148**, 83–92.

EYIDOĞAN, H. & JACKSON, J. 1985. A seismological study of normal faulting in the Demirci, Alasehir and Gediz earthquakes of 1969–70 in western Turkey: implication for the nature and geometry of deformation in the continental crust. *Geophysical Journal of the Royal Astronomical Society* **81**, 569–607.

FAURE, M., BONNEAU, M. & PONS, J. 1991. Ductile deformation and syntectonic granite emplacement during the late Miocene extension of the Aegean (Greece). *Bulletin de la Société Geologique de France* **162**, 3–11.

GAUTIER, P., BRUN, J.-P. & JOLIVET, L. 1993. Structure and kinematics of upper Cenozoic extensional detachment on Naxos and Paros (Cyclades Islands, Greece). *Tectonics* **12**, 1180–94.

GESSNER, K., COLLINS, A. S., RING, U. & GÜNGÖR, T. 2004. Structural and thermal history of poly-orogenic basement; U–Pb geochronology of granitoid rocks in the southern Menderes Massif, western Turkey. *Journal of the Geological Society, London* **161**, 93–101.

GESSNER, K., PIAZOLO, S., GÜNGÖR, T., RING, U., KRÖNER, A. & PASSCHIER, C. W. 2001*a*. Tectonic significance of deformation patterns in granitoid rocks of the Menderes nappes, Anatolide belt, southwest Turkey. *International Journal of Earth Sciences* **89**, 766–80.

GESSNER, K., RING, U., JOHNSON, C., HETZEL, R., PASSCHIER, C. W. & GÜNGÖR, T. 2001*b*. An active bivergent rolling-hinge detachment system: The central Menderes metamorphic core complex in western Turkey. *Geology* **29**, 611–14.

GESSNER, K., RING, U., PASSCHIER, C. W. & GÜNGÖR, T. 2001*c*. How to resist subduction: evidence for large-scale out-of-sequence thrusting during Eocene collision in western Turkey. *Journal of the Geological Society, London* **158**, 769–84.

GETTY, S. R. & GROMET, L. P. 1992. Geochronological constraints on ductile deformation, crustal extension, and doming about a basement-cover boundary, New England, Appalachians. *American Journal of Science* **292**, 359–97.

GOKTEN, E., HAVZOĞLU, T. & ŞAN, Ö. 2001. Tertiary evolution of the central Menderes Massif based on structural investigations of metamorphics and sedimentary cover rocks between Salihli and Kiraz (western Turkey). *International Journal of Earth Sciences* **89**, 745–56.

GROVE, M. & HARRISON, T. M. 1996. $^{40}Ar^{*}$ diffusion in Fe-rich biotite. *American Mineralogist* **81**, 940–51.

HENJES-KUNST, F., ALTHERR, R., KREUZER, H. & HANSEN, B. T. 1988. Disturbed U–Pb systematics of young zircons and uranothorites: The case of the Miocene Aegean granitoids (Greece). C*hemical Geology* **73**, 125–45.

HETZEL, R., PASSCHIER, C. W., RING, U. & DORA, Ö. O. 1995*a*. Bivergent extension in orogenic belts: The Menderes massif (southwestern Turkey). *Geology* **23**, 455–8.

HETZEL, R., RING, U., AKAL, C. & TROESCH, M. 1995*b*. Miocene NNE–directed extensional unroofing in the Menderes Massif, southwestern Turkey. *Journal of the Geological Society, London* **152**, 639–54.

ILKIŞIK, O. M. 1995. Regional heat flow in western Anatolia using silica temperature estimates from thermal springs. *Tectonophysics* **244**, 175–84.

IŞIK, V., SEYITOĞLU, G. & ÇEMEN, I. 2003. Ductile–brittle transition along the Alaşehir detachment fault and its structural relationship with the Simay detachment fault, Menderes massif, western Turkey. *Tectonophysics* **374**, 1–18.

IŞIK, V. & TEKELI, O. 2001. Late orogenic crustal extension in northern Menderes Massif (western Turkey): evidence for metamorphic core complex formation. *International Journal of Earth Sciences* **89**, 757–65.

IŞIK, V., TEKELI, O. & SEYITOĞLU, G. 2004. The $^{40}Ar/^{39}Ar$ age of extensional ductile deformation and granitoid intrusion in the northern Menderes core complex: implications for the initiation of extensional tectonics in western Turkey. *Journal of Asian Earth Sciences* **23**, 555–66.

KEAY, S., LISTER, G. & BUICK, I. 2001. The timing of partial melting, Barrovian metamorphism and granite intrusion in the Naxos metamorphic core complex, Cyclades, Aegean Sea, Greece. *Tectonophysics* **342**, 275–312.

KOÇYIĞIT, A., YUSUFOĞLU, H. & BOZKURT, E. 1999. Evidence from the Gediz graben for episodic two-stage extension in western Turkey. *Journal of the Geological Society, London* **156**, 605–16.

KUMERICS, C., RING, U., BRICHAU, S., GLODNY, J. & MONIÉ, P. 2005. The extensional Messaria shear zone and associated brittle detachment faults, Aegean Sea, Greece. *Journal of the Geological Society, London* **162**, 701–21.

LARSON, T. E. & SHARP, Z. D. 2003. Stable isotope constraints on the Al_2SiO_5 'triple-point' rocks from the Proterozoic Priest pluton contact aureole, New Mexico, USA. *Journal of Metamorphic Geology* **21**, 785–98.

LIPS, A. L. W., CASSARD, D., SÖZBILIR, H., YILMAZ, H. & WIJBRANS, J. R. 2001. Multistage exhumation of the Menderes Massif, western Anatolia (Turkey). *International Journal of Earth Sciences* **89**, 781–92.

LISTER, G. S., BANGA, G. & FEENSTRA, A. 1984. Metamorphic core complexes of Cordilleran type in the Cyclades, Aegean Sea, Greece. *Geology* **12**, 221–5.

LOOS, S. & REISCHMANN, T. 1999. The evolution of the southern Menderes Massif in SW Turkey as revealed by zircon dating. *Journal of the Geological Society, London* **156**, 1021–30.

LUDWIG, K. R. 1980. Calculation of uncertainties of U–Pb isotope data. *Earth and Planetary Science Letters* **46**, 212–20.

LUDWIG, K. R. 1993. PBDAT – a computer program for processing Pb–U–Th isotope data, Version 1. 24. *US Geological Survey open-file report* **88–542**, 1–33.

LUDWIG, K. R. 1999. Isoplot/Ex Ver 2. 06: A geochronological toolkit for Microsoft Excel. *Berkeley Geochronology Center Special Publications*, 1a.

MCCLUSKY, S. & 14 OTHERS. 2000. Global Positioning System constraints on plate kinematics and dynamics in the eastern Mediterranean and Caucasus. *Journal of Geophysical Research* **105**, 5695–719.

OBERHÄNSLI, R., CANDAN, O., DORA, O. O. & DÜRR, S. H. 1997. Eclogites within the Menderes Massif/western Turkey. *Lithos* **41**, 135–50.

OBERLI, F., MEIER, M., BERGER, A., ROSENBERG, C. L. & GIERÉ, R. 2004. U–Th–Pb and $^{230}Th/^{238}U$ disequilibrium isotope systematics: precise accessory mineral chronology and melt evolution tracing in the Alpine Bergell intrusion. *Geochimica et Cosmochimica Acta* **68**, 2543–60.

PATON, S. 1992. Active normal faulting, drainage patterns and sedimentation in southwestern Turkey. *Journal of the Geological Society, London* **149**, 1031–44.

PE-PIPER, G., KOUKOUVELAS, I. & PIPER, D. J. W. 1998. Synkinematic granite emplacement in a shear zone; the Pleasant Hills Pluton, Canadian Appalachians. *Geological Society of America Bulletin* **110**, 523–36.

PE-PIPER, G., PIPER, D. J. W. & MATARANGAS, D. 2002. Regional implications of geochemistry and style of emplacement of Miocene I-type diorite and granite, Delos, Cyclades, Greece. *Lithos* **60**, 47–66.

PURVIS, M. & ROBERTSON, A. 2004. A pulsed extension model for the Neogene–Recent E–W-trending Alasehir Graben and the NE–SW-trending Selendi and Gördes Basins, western Turkey. *Tectonophysics* **391**, 171–201.

PURVIS, M. & ROBERTSON, A. 2005*a*. Miocene sedimentary evolution of the NE–SW-trending Selendi and Gördes basins, W Turkey: implications for extensional processes. *Sedimentary Geology* **174**, 31–62.

PURVIS, M. & ROBERTSON, A. 2005*b*. Sedimentation of the Neogene–Recent Alaşehir (Gediz) continental graben system used to test alternative tectonic models for western (Aegean) Turkey. *Sedimentary Geology* **173**, 373–408.

RAHL, J. M., MCGREW, A. J. & FOLAND, K. A. 2002. Transition from Contraction to Extension in the Northeastern Basin and Range: New Evidence from the Copper Mountains, Nevada. *Journal of Geology* **110**, 179–94.

REDDY, S. M. & POTTS, G. J. 1999. Constraining absolute deformation ages: the relationship between deformation mechanisms and isotope systematics. *Journal of Structural Geology* **21**, 1255–65.

RING, U. & COLLINS, A. S. 2005. U–Pb SIMS dating of synkinematic granites: Timing of core-complex formation in the northern Anatolide belt of western Turkey. *Journal of the Geological Society, London* **162**, 289–98.

RING, U., GESSNER, K., GÜNGÖR, T. & PASSCHIER, C. W. 1999. The Menderes belt of western Turkey and the Cycladic belt in the Aegean – do they really correlate? *Journal of the Geological Society, London* **156**, 3–6.

RING, U., JOHNSON, C., HETZEL, R. & GESSNER, K. 2003. Tectonic denudation of a Late Cretaceous–Tertiary collisional belt: regionally symmetric cooling patterns and their relation to extensional faults in the Anatolide belt of western Turkey. *Geological Magazine* **140**, 421–41.

ROMER, R. & SIEGESMUND, S. 2003. Why allanite may swindle about its true age. C*ontributions to Mineralogy and Petrology* **146**, 297–307.

SCHÄRER, U. 1984. The effect of initial ^{230}Th disequilibrium on young U–Pb ages: the Makalu case, Himalaya. *Earth and Planetary Science Letters* **67**, 191–204.

ŞENGÖR, A. M. C. 1987. Cross faults and differential stretching in their hanging walls in regions of low-angle normal faulting: examples from western Turkey. In *Continental extensional tectonics* (eds M. J. Coward, J. F. Dewey and P. L. Hancock), pp. 405–73. Geological Society of London, Special Publication no. 28.

ŞENGÖR, A. M. C., SATIR, M. & AKKÖK, R. 1984. Timing of tectonic events in the Menderes Massif, western Turkey: implications for tectonic evolution and evidence for Pan-African basement in Turkey. *Tectonics* **3**, 693–707.

SEYITOĞLU, G., ÇEMEN, I. & TEKELI, O. 2000. Extensional folding in the Alasehir (Gediz) graben, western Turkey. *Journal of the Geological Society, London* **157**, 1097–1100.

SEYITOĞLU, G., IŞIK, V. & ÇEMEN, I. 2004. Complete Tertiary exhumation history of the Menderes massif, western Turkey: an alternative working hypothesis. *Terra Nova* **16**, 358–64.

SEYITOĞLU, G. & SCOTT, B. C. 1996. The age of the Alaşehir graben (west Turkey) and its tectonic implications. *Geological Journal* **31**, 1–11.

SEYITOĞLU, G., SCOTT, B. C. & RUNDLE, C. C. 1992. Timing of Cenozoic extensional tectonics in west Turkey. *Journal of the Geological Society, London* **149**, 533–8.

SEYITOĞLU, G., TEKELI, O., ÇEMEN, I., ŞEN, S. & IŞIK, V. 2002. The role of the flexural rotation/rolling hinge model in the tectonic evolution of the Alaşehir graben, western Turkey. *Geological Magazine* **139**, 15–26.

THOMSON, S. & RING, U. 2006. Thermochronologic evaluation of post-collision extension in the Anatolide orogen, western Turkey. *Tectonics* **25**(3), TC3005, doi: 10.1029/2005TC001833.

VANCE, D., MÜLLER, W. & VILLA, I. M. (eds) 2003. *Geochronology: linking the isotopic record with petrology and textures*. Geological Society of London, Special Publication no. 220, 260 pp.

VILLA, I. M. 1998. Isotopic closure. *Terra Nova* **10**, 42–7.

VILLA, I. M. & PUXEDDU, M. 1994. Geochronology of the Larderello geothermal field: new data and the 'closure temperature' issue. *Contributions to Mineralogy and Petrology* **115**, 415–26.

WESTAWAY, R. 1996. Comment on 'Bivergent extension in orogenic belts: the Menderes Massif (southwestern Turkey)' by R. Hetzel, C. W. Passchier, U. Ring, and Ö. O. Dora. *Geology* **24**, 93–4.

WESTAWAY, R. 2006. Cenozoic cooling histories in the Menderes Massif, western Turkey, may be caused by erosion and flat subduction, not low angle normal faulting. *Tectonophysics* **412**, 1–25.

WESTAWAY, R., PRINGLE, M., YURTMEN, S., DEMIR, T., BRIDGLAND, D., ROWBOTHAM, G. & MADDY, D. 2004. Pliocene and Quaternary regional uplift in western Turkey: the Gediz river terrace staircase and the volcanism at Kula. *Tectonophysics* **391**, 121–69.

WIJBRANS, J. R. & MCDOUGALL, I. 1988. ^{39}Ar/^{40}Ar dating of white micas from an alpine high-pressure metamorphic belt on Naxos (Greece): the resetting of the argon isotopic system. *Contribution to Mineralogy and Petrology* **93**, 187–94.

YILMAZ, M. & GELISLI, K. 2003. Stratigraphic-structural interpretation and hydrocarbon potential of the Alaşehir Graben, western Turkey. *Petroleum Geoscience* **9**, 277–82.

YILMAZ, Y., GENÇ, S. C., GÜRER, F., BOZCU, M., YILMAZ, K., KARACIK, Z., ALTUNKAYNAK, Ş. & ELMAS, A. 2000. When did the western Anatolian grabens begin to develop? In *Tectonics and magmatism in Turkey and surrounding regions* (eds E. Bozkurt, J. A. Winchester and J. D. A. Piper.), pp. 353–84. Geological Society of London, Special Publication no. 173.

YILMAZ, Y., GENÇ, S. C., KARACIK, Z. & ALTUNKAYNAK, Ş. 2001. Two contrasting magmatic associations of NW Anatolia and their tectonic significance. *Journal of Geodynamics* **31**, 243–71.